

MYELOID NEOPLASIA

Molecular taxonomy of myelodysplastic syndromes and its clinical implications

Elsa Bernard,^{1,2} Robert P. Hasserjian,³ Peter L. Greenberg,⁴ Juan E. Arango Ossa,¹ Maria Creignou,⁵ Heinz Tuechler,⁶ Jesus Gutierrez-Abriol,¹ Dylan Domenico,¹ Juan S. Medina-Martinez,¹ Max Levine,¹ Konstantinos Liosis,¹ Noushin Farnoud,¹ Maria Sirenko,¹ Martin Jädersten,⁵ Ulrich Germing,⁷ Guillermo Sanz,^{8,9} Arjan A. van de Loosdrecht,¹⁰ Yasuhito Nannya,¹¹ Olivier Kosmider,¹² Matilde Y. Follo,¹³ Felicitas Thol,¹⁴ Lurdes Zamora,^{15,16} Ronald F. Pinheiro,¹⁷ Andrea Pellagatti,¹⁸ Harold K. Elias,¹⁹ Detlef Haase,²⁰ Christina Ganster,²⁰ Lionel Ades,²¹ Magnus Tobianson,⁵ Laura Palomo,^{15,16} Matteo Giovanni Della Porta,²² Pierre Fenaux,²¹ Monika Belickova,²³ Michael R. Savona,²⁴ Virginia M. Klimek,¹⁹ Fabio P. S. Santos,²⁵ Jacqueline Boulwood,¹⁸ Ioannis Kotsianidis,²⁶ Valeria Santini,²⁷ Francesc Solé,¹⁶ Uwe Platzbecker,²⁸ Michael Heuser,¹⁴ Peter Valent,^{29,30} Carlo Finelli,³¹ Maria Teresa Voso,³² Lee-Yung Shih,³³ Michaela Fontenay,¹² Joop H. Jansen,³⁴ José Cervera,³⁵ Norbert Gattermann,⁷ Benjamin L. Ebert,³⁶ Rafael Bejar,³⁷ Luca Malcovati,^{38,39} Seishi Ogawa,^{11,40} Mario Cazzola,^{38,39} Eva Hellström-Lindberg,⁵ and Elli Papaemmanuil¹

¹Department of Epidemiology and Biostatistics, Memorial Sloan Kettering Cancer Center, New York, NY; ²Department of Computational Oncology, UMR 981, Gustave Roussy, Villejuif, France; ³Department of Pathology, Massachusetts General Hospital, Boston, MA; ⁴Division of Hematology, Stanford University Cancer Institute, Stanford, CA; ⁵Department of Medicine Huddinge, Center for Hematology and Regenerative Medicine, Karolinska Institutet, Karolinska University Hospital, Stockholm, Sweden; ⁶Independent Researcher, Vienna, Austria; ⁷Department of Hematology, Oncology, and Clinical Immunology, Heinrich Heine University, Düsseldorf, Germany; ⁸Department of Hematology, Hospital Universitario y Politécnico La Fe, Valencia, Spain; ⁹Centro de Investigación Biomédica en Red Cáncer, Instituto de Salud Carlos III, Madrid, Spain; ¹⁰Department of Hematology, Amsterdam University Medical Center, Vrije University Medical Center, Amsterdam, The Netherlands; ¹¹Department of Pathology and Tumor Biology, Kyoto University, Kyoto, Japan; ¹²Department of Hematology, Assistance Publique-Hôpitaux de Paris, Hôpital Cochin and Université de Paris, Université Paris Descartes, Paris, France; ¹³Department of Biomedical and Neuromotor Sciences, University of Bologna, Bologna, Italy; ¹⁴Department of Hematology, Hemostasis, Oncology, and Stem Cell Transplantation, Hannover Medical School, Hannover, Germany; ¹⁵Hematology Department, Catalan Institute of Oncology, Hospital Germans Trias i Pujol, Barcelona, Spain; ¹⁶Myelodysplastic Syndromes Group, Josep Carreras Leukemia Research Institute, Barcelona, Spain; ¹⁷Drug Research and Development Center, Federal University of Ceara, Ceara, Brazil; ¹⁸Radcliffe Department of Medicine, Nuffield Division of Clinical Laboratory Sciences, University of Oxford, Oxford, United Kingdom; ¹⁹Department of Medicine, Memorial Sloan Kettering Cancer Center, New York, NY; ²⁰Clinics of Hematology and Medical Oncology, University Medical Center, Göttingen, Germany; ²¹Department of Hematology, Hôpital St Louis, and Paris University, Paris, France; ²²Department of Biomedical Sciences, Humanitas Clinical and Research Center and Humanitas University, Milan, Italy; ²³Department of Genomics, Institute of Hematology and Blood Transfusion, Prague, Czech Republic; ²⁴Department of Medicine, Vanderbilt-Ingram Cancer Center, Vanderbilt University School of Medicine, Nashville, TN; ²⁵Oncology-Hematology Center, Hospital Israelita Albert Einstein, São Paulo, Brazil; ²⁶Department of Hematology, University Hospital of Alexandroupolis, Democritus University of Thrace, Alexandroupolis, Greece; ²⁷Myelodysplastic Syndromes Unit, Department of Experimental and Clinical Medicine, Hematology, Azienda Ospedaliero Universitaria Careggi, University of Florence, Florence, Italy; ²⁸Medical Clinic and Policlinic 1, Hematology and Cellular Therapy, University of Leipzig, Leipzig, Germany; ²⁹Division of Hematology and Hemostaseology, Department of Internal Medicine I, Ludwig Boltzmann Institute for Hematology and Oncology, and ³⁰Department of Internal Medicine I, Ludwig Boltzmann Institute for Hematology and Hemostaseology, Medical University of Vienna, Vienna, Austria; ³¹Institute of Hematology Seragnoli, Istituti di Ricovero e Cura a Carattere Scientifico Azienda Ospedaliero-Universitaria di Bologna, Bologna, Italy; ³²Myelodysplastic Syndromes Cooperative Group Gruppo Laziale Mielodisplasie (GROM-L), Department of Biomedicine and Prevention, Tor Vergata University, Rome, Italy; ³³Division of Hematology, Chang Gung Memorial Hospital at Linkou, Chang Gung University, Taoyuan City, Taiwan; ³⁴Laboratory of Hematology, Department of Laboratory Medicine, Radboud University Medical Centre, Nijmegen, The Netherlands; ³⁵Department of Hematology and Genetics Unit, University Hospital La Fe, Valencia, Spain; ³⁶Department of Medical Oncology and Howard Hughes Medical Institute, Dana-Farber Cancer Center, Boston, MA; ³⁷University of California San Diego Moores Cancer Center, La Jolla, CA; ³⁸Department of Hematology Oncology, Fondazione Istituto di Ricovero e Cura a Carattere Scientifico Policlinico San Matteo, Pavia, Italy; ³⁹Department of Molecular Medicine, University of Pavia, Pavia, Italy; and ⁴⁰Institute for the Advanced Study of Human Biology, Kyoto University, Kyoto, Japan

KEY POINTS

- Genomic profiling identifies molecular subgroups of MDS associated with distinct clinical phenotypes and disease courses.
- The molecular taxonomy is a basis for a mechanistic MDS classification that might benefit clinical decision-making and therapeutic research.

Myelodysplastic syndromes (MDS) are clonal hematologic disorders characterized by morphologic abnormalities of myeloid cells and peripheral cytopenias. Although genetic abnormalities underlie the pathogenesis of these disorders and their heterogeneity, current classifications of MDS rely predominantly on morphology. We performed genomic profiling of 3233 patients with MDS or related disorders to delineate molecular subtypes and define their clinical implications. Gene mutations, copy-number alterations, and copy-neutral loss of heterozygosity were derived from targeted sequencing of a 152-gene panel, with abnormalities identified in 91%, 43%, and 11% of patients, respectively. We characterized 16 molecular groups, encompassing 86% of patients, using information from 21 genes, 6 cytogenetic events, and loss of heterozygosity at the *TP53* and *TET2* loci. Two residual groups defined by negative findings (molecularly not otherwise specified, absence of recurrent drivers) comprised 14% of patients. The groups varied in size from 0.5% to 14% of patients and were associated with distinct clinical phenotypes and

outcomes. The median bone marrow (BM) blast percentage across groups ranged from 1.5% to 10%, and the median overall survival ranged from 0.9 to 8.2 years. We validated 5 well-characterized entities, added further evidence to support 3 previously reported subsets, and described 8 novel groups. The prognostic influence of BM blasts depended on the genetic subtypes. Within genetic subgroups, therapy-related MDS and myelodysplastic/myeloproliferative neoplasms had comparable clinical and outcome profiles to primary MDS. In conclusion, genetically-derived subgroups of MDS are clinically relevant and might inform future classification schemas and translational therapeutic research.

Introduction

Myelodysplastic syndromes (MDS) comprise a diverse group of myeloid neoplasms characterized by morphologic dysplasia, persistent cytopenias, and a variable risk of evolution to acute myeloid leukemia (AML).¹ More than 50 genes are recurrently mutated in MDS implicating the spliceosome complex, epigenetic or transcriptional modifiers, and signaling pathways.^{2,3} Genomic profiling efforts have demonstrated preferred comutation patterns and robust associations between gene mutations and clinical presentation.²⁻⁷

With current classification schemas relying predominantly on bone marrow (BM) morphology, clinical phenotypes within MDS diagnostic categories exhibit significant heterogeneity.⁸⁻¹⁰ This highlights the need for defining genetically-informed disease subtypes to better understand MDS pathogenesis and the variability in responses to treatment and outcomes observed in patients. However, the complexity of the MDS genetic landscape has challenged the delineation of genetic subtypes.⁶ Formalizing the definition of genetic subtypes would provide a valuable tool for future studies focused on elucidating disease mechanisms and therapeutic targeting.

In this work, we studied how genetic alterations delineate specific disease subtypes using 3233 representative samples from patients with MDS from the cohort built to develop the International Prognostic Scoring System Molecular (IPSS-M).⁷ We analyzed comutation patterns and genotype-phenotype associations for gene mutations, copy-number alterations (CNAs), and copy-neutral loss of heterozygosity (cnLOH) events. Patients were clustered based on their composite molecular profiles to develop a molecular taxonomy comprising 18 different groups (16 molecular groups and 2 residual groups). The clinical implications of the proposed MDS molecular taxonomy were evaluated.

Methods

Study cohort

The cohort consisted of 3233 treatment-naive diagnostic BM or blood samples from adult patients (median age, 72 years) with MDS or related neoplasms with <30% blasts per the World Health Organization (WHO) 2016 classification (excluding AML with recurrent genetic abnormalities; ie, AML-defining cytogenetic lesions, *NPM1*, or *CEBPA* mutations; supplemental Tables 1-3,⁸ available on the *Blood* website). To enable the study of molecular subtypes across the borders of diagnostic entities, we included 536 patients with myelodysplastic/myeloproliferative neoplasms (MDS/MPN; 371 and 165 with

white blood cell [WBC] count below or above $13 \times 10^9/L$, respectively), 267 patients with secondary/therapy-related MDS (s/t-MDS), and 85 patients with AML (61 AML with myelodysplasia-related changes, and 24 AML not otherwise specified). Clinical annotation, cytogenetic, and outcome data were recorded. WHO 2016, WHO 2022, and International Consensus Classification (ICC) classifications were assigned (supplemental Table 4).⁸⁻¹⁰ Diagnostic subtypes defined by genetic biomarkers (MDS-5q, MDS-SF3B1, or MDS-biTP53) represented 23% and 22% of cases per WHO 2022 and ICC, respectively.

The study was approved by the institutional review board and Memorial Sloan Kettering Cancer Center after full consideration of the scope and methods of the study.

Genomic analysis

Sequencing was performed with a targeted 152-gene panel enriched with genome-wide CNA probes. Oncogenic mutations with a minimum variant allele frequency (VAF) of 2% were considered. Arm-level CNAs and cnLOH events were called using CNACS,¹¹ complementing cytogenetic. The putative cancer cell fraction per sample was inferred as twice the maximum VAF adjusted for ploidy. Whole-genome sequencing was performed on 30 samples. For further details see the supplemental Methods.

Statistical analysis

Molecular features were constructed from the presence or absence of genetic alterations (gene mutations, CNAs, and cnLOH events). Comutation analysis or prior knowledge further informed the derivation of specific features encoding distinct allelic states or hot spot mutations.^{12,13} The molecular features were used as input for unsupervised clustering analysis using Bayesian Dirichlet processes to identify genetic groups with high within-group similarity and between-group discrimination.¹³ The results were then manually curated into a rule-based hierarchical classification tree. The relative chronological order of gene mutations was inferred through Bradley-Terry analysis.² The IPSS-M score and risk categories were calculated using the open-access R package.^{7,14}

Results

Integrative comutation patterns and implications for genotype-phenotype analysis

We characterized 10 564 oncogenic mutations across 126 genes in 91% of patients, 3558 chromosomal alterations in 43% of patients, and 375 cnLOH events in 11% of patients (Figure 1A). Gene mutation and CNA comutation patterns were consistent with prior studies (supplemental Figure 1).^{2-4,15-17}

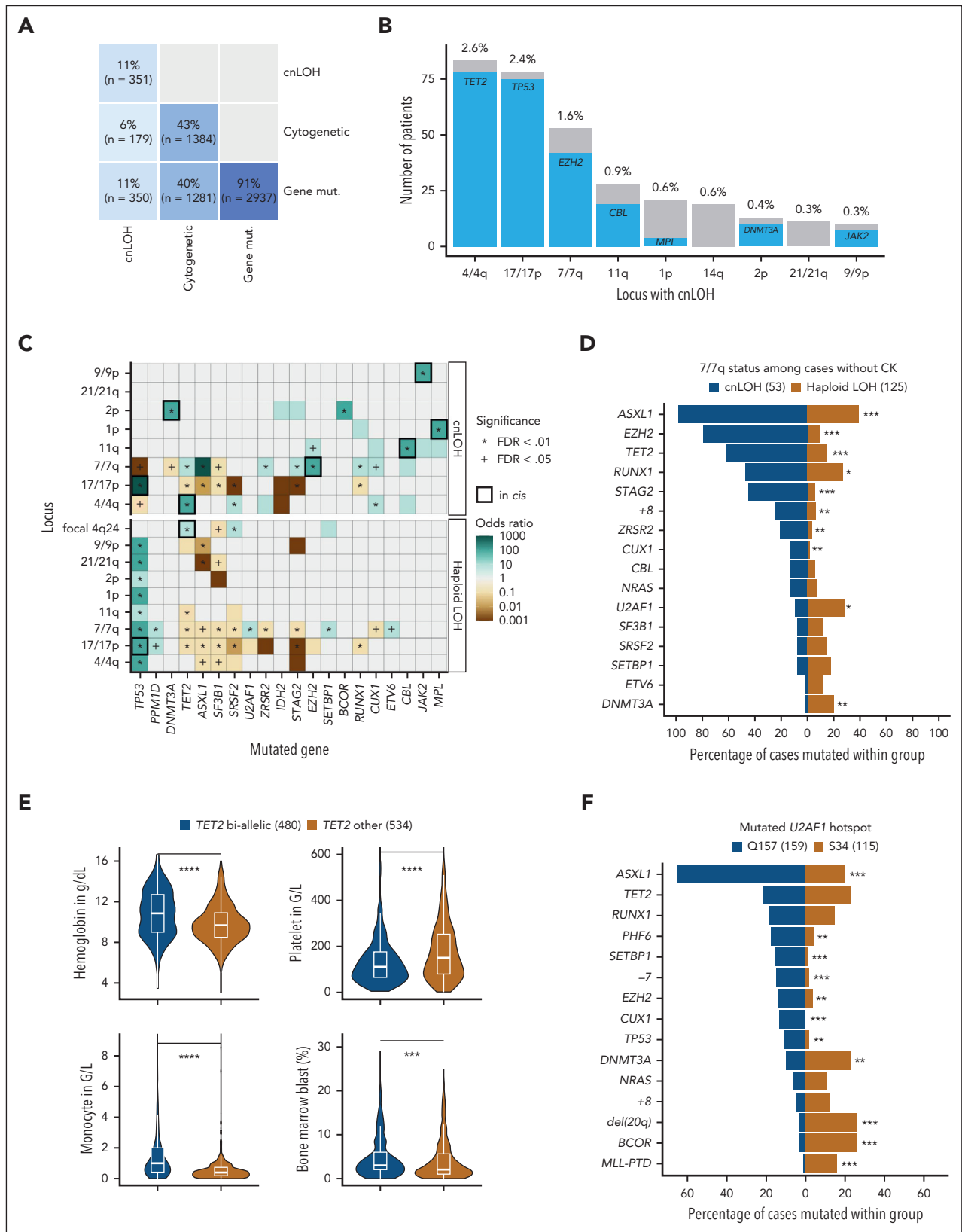


Figure 1. Integrative comutation patterns in MDS and implications for genotype-phenotype analysis. (A) Proportion and number of patients with or without gene mutations (mut.), cytogenetic alterations, and cnLOH events. (B) Number of patients with cnLOH at the most recurrent loci and co-occurrence of gene mutations in cis. The most recurrent cnLOH loci were 4/4q (2.6%), 17/17p (2.3%), and 7/7q (1.6%). Mutations in *TET2*, *TP53*, and *EZH2* occurred in 94% (78/83), 96% (75/78), and 79% (42/53) of cases with cnLOH at the 4/4q, 17/17p, and 7/7q loci, respectively. (C) Heat map representing mutual exclusivity (brown) or co-occurrence (green) between gene mutations and loci with haploid LOH or cnLOH. Apart from the strong cnLOH–gene mutation interaction in cis (black thick line), focal deletions at the *TET2* locus (4q24) also co-occurred with *TET2* mutations (OR, 2.4; $P = .0007$). P values are from Fisher exact test with Benjamini-Hochberg (BH) multiple testing correction. (D) Comparison of comutation frequencies

Interactions in cis between gene mutation and cnLOH Of the patients with cytogenetic or cnLOH alterations, 93% (1281/1384) and 99% (350/351) had co-occurring gene mutations, respectively (Figure 1A). The interactions between cnLOH events and gene mutations in cis were highly specific, most frequently 4q-TET2, 17p-TP53, and 7q-EZH2 (odds ratio [OR], 37, 247, and 68, respectively; $P < .0001$), but also 11q-CBL, 2p-DNMT3A, 9p-JAK2, and 1p-MPL (Figures 1B-C). Large chromosomal losses (haploid LOH) but not cnLOH events were systematically linked to TP53 mutations (Figure 1C). Haploid LOH and cnLOH events had distinct genome-wide comutation patterns (Figure 1D). As observed in clonal hematopoiesis,^{18,19} cnLOH events likely contribute to biallelic inactivation and/or allele dosage adjustment of specific mutated genes in MDS.²⁰

TET2 allelic states are associated with distinct comutation patterns and clinical correlates Consistent with published methodology,^{12,21} we integrated the number of TET2 mutations, their cumulative VAFs, and 4q24 LOH status to stratify 1014 patients with mutated TET2 into 2 groups: (1) "TET2 biallelic" (47%), and (2) "TET2 other" (53%) representing likely monoallelic mutation (supplemental Figure 2). SRSF2 mutations were more frequent in the TET2 biallelic group, whereas SF3B1 mutations prevailed in TET2 other (OR, 2.7 and 0.45, respectively; $P < .0001$; supplemental Figure 3). Chronic myelomonocytic leukemia (CMML) was enriched in the biallelic group (38% vs 9%; OR, 6.4; $P < .0001$). Blood counts and BM blast percentages differed between the 2 TET2 subsets (Figure 1E), but not overall survival (OS; supplemental Figure 3).

Distinct comutation patterns between U2AF1 hot spot mutations We systematically assessed comutation patterns across hot spot mutations within genes. Among 278 patients with mutated U2AF1, 58% had a Q157 mutation, 41% had a S34 mutation, and 1% had both. Patients with Q157 or S34 mutations had distinct comutation patterns (Figure 1F), in addition to previously reported different RNA splicing events.^{22,23} However, their clinical profiles were similar (supplemental Figure 4). For SF3B1 hot spot mutations, the only significant difference was an overrepresentation of STAG2 mutations in patients with K666 mutation, with no other clear clinical associations (supplemental Figure 4).^{24,25}

Together, these results emphasize the importance of incorporating cnLOH events, allelic states, and hot spot mutations to study genetic subtypes. Such discrimination lacked in recent prior MDS molecular classification studies.^{5,26}

Derivation of MDS molecular subgroups and their clinical relevance

We characterized 18 molecular subgroups using unequivocal and hierarchical rules (Figure 2; supplemental Figure 5). The first

16 groups (86%, $n = 2769$) were based on the presence of mutations in 21 genes (ASXL1, BCOR, BCORL1, DDX41, DNMT3A, EZH2, FLT3, IDH1, IDH2, MLL [ie, KMT2A], MYC, NPM1, SETBP1, SF3B1, SRSF2, STAG2, TET2, TP53, U2AF1, WT1, and ZRSR2), 6 cytogenetic events (inv(3), complex karyotype [CK], der(1;7), -7, del(5q), -Y), and LOH at the TP53 and TET2 loci. The molecularly not otherwise specified (mNOS) group (8%, $n = 254$) corresponded to the presence of other cytogenetic abnormalities and/or mutations in 51 other recurrently mutated genes (>0.5%). The No-event category (6%, $n = 210$) was characterized by the absence of any recurrent drivers evaluated in this study.

The groups varied in size (0.5%-14%) and in molecular complexity (median, 0-5 mutated genes per patient; Figure 3; supplemental Figures 6-7; supplemental Table 5). They were associated with distinct demographics, clinical presentations, and patient outcomes (Figure 3; Figure 4A-B; supplemental Figures 8-11). Median age of diagnosis across groups ranged from 64 to 75 years, median BM blast percentage ranged from 1.5% to 10%, median OS ranged from 0.9 to 8.2 years, and 2-year rate of leukemic transformation ranged from 0% to 40%. The IPSS-M captured genetic heterogeneity in relation to outcomes within molecular groups (Figure 3) and retained superior predictive performances compared with a model based on molecular groups, consistent with prior studies (supplemental Figure 12).⁵

From the 16 groups excluding mNOS and No-event groups (accounting together for 14% of patients), 5 subgroups (36%, $n = 1176$) validated established (TP53-complex, del(5q), and SF3B1) or well-characterized entities (DDX41 and AML-like; supplemental Figures 13-19), 3 subgroups (20%, $n = 651$) supported previously reported subsets (bi-TET2, der(1;7), and CCUS-like; supplemental Figures 20-22), and 8 subgroups were novel (30%, $n = 942$; supplemental Figures 23-28).

Established or well-characterized entities: DDX41, AML-like, TP53-complex, del(5q), and SF3B1

The DDX41 group (3.3%, $n = 107$; supplemental Figure 13) aligned with the results of Makishima et al.²⁷ In our study, 56% of patients with mutated DDX41 had both a putative germ line DDX41 variant (defined here as >30% VAF) and a somatic DDX41 mutation, 37% only a putative germ line DDX41 variant, and 7% only somatic DDX41 mutations (≥ 1 ; supplemental Table 6). DDX41 mutations were the sole alteration in 23% of cases, more frequently biallelic than monoallelic (16 and 9 cases, respectively). CUX1 was the only gene significantly comutated with DDX41 (OR, 3.4; $P < .001$). TET2 mutations were mutually exclusive with biallelic but not monoallelic DDX41 mutations ($P = .0003$). The DDX41 group had a unique

Figure 1 (continued) between cases with cnLOH (blue) or haploid LOH (gold) at 7/7q in the absence of CK. For example, mutations in EZH2 were enriched in the 53 cases with cnLOH at 7/7q (79%) compared with the 125 cases with isolated haploid LOH at 7/7q (10%). Conversely, haploid LOH at 7/7q was significantly enriched for U2AF1 and DNMT3A mutations (28% and 20%) compared with cnLOH at 7/7q (9% and 2%). P values are from Fisher exact test with BH multiple testing correction. *** $P < .001$; ** $P < .01$; * $P < .05$. (E) Comparison of the distributions of blood counts and of the percentage of BM blasts between cases classified as TET2 biallelic (blue) or TET2 other (ie, likely monoallelic, gold). P values are from the Wilcoxon rank-sum test. **** $P < .0001$; *** $P < .001$. (F) Comparison of comutation frequencies between cases with U2AF1 Q157 or S34 hot spot mutations. For example, ASXL1 mutations were present in 65% and 20% of patients with U2AF1 Q157 and S34 mutations, respectively (OR, 7.3; $P < .0001$). Mutations in CUX1, EZH2, PHF6, SETBP1, TP53, and monosomy 7 were also significantly more frequent in the Q157 subset. Conversely, BCOR mutations and del(20q) were more common in patients with S34 (26%) compared with Q157 (3%) mutations ($P < .0001$). P values are from Fisher exact test with BH multiple testing correction. *** $P < .001$; ** $P < .01$. FDR, false discovery rate; PTD, partial tandem duplication.

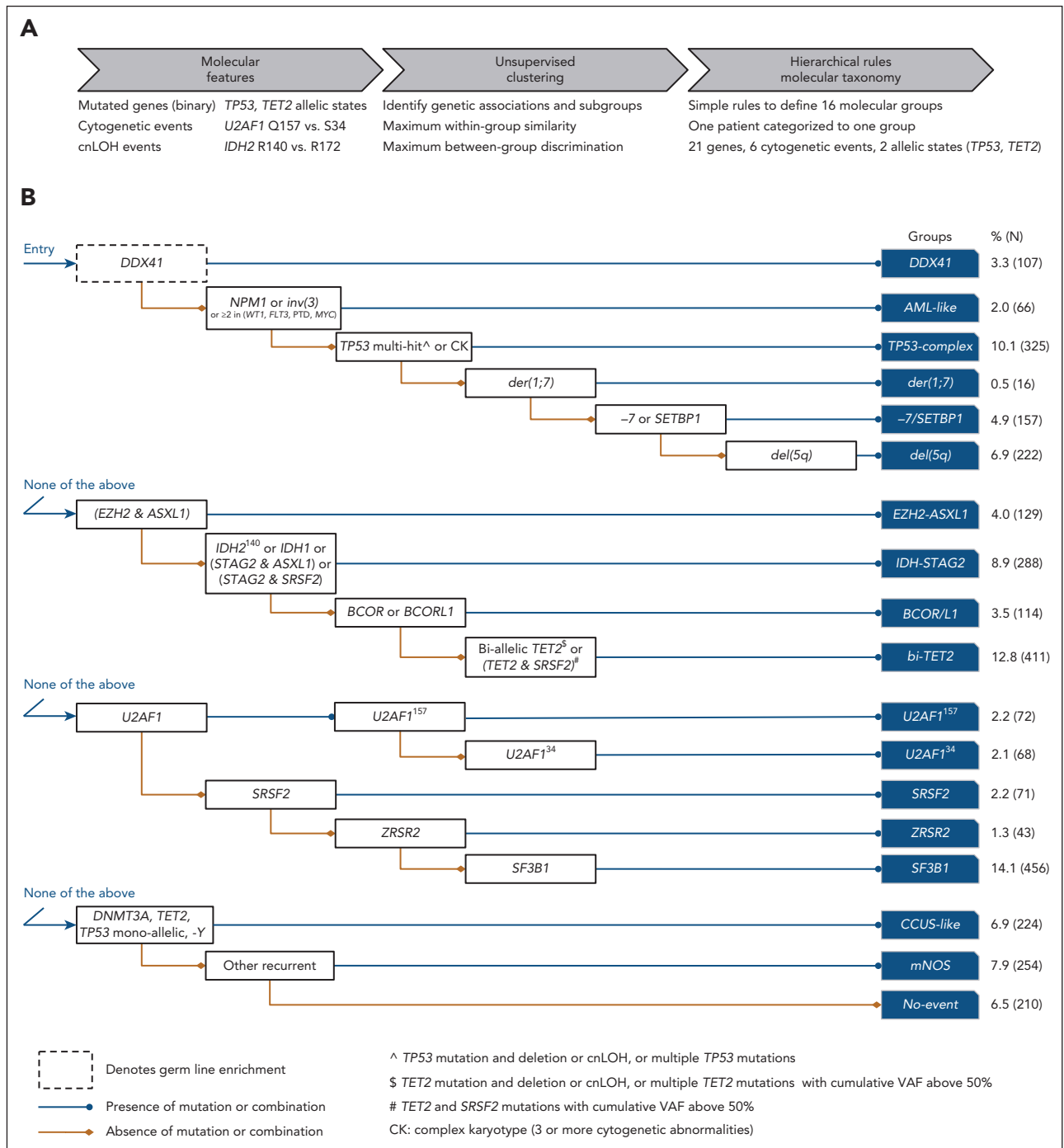


Figure 2. Derivation of 16 MDS molecular groups. (A) Schematic of the analytical workflow to identify molecular groups. Features were based on the presence or absence of genetic alterations (gene mutations, cytogenetic, and cnLOH events). Distinct allelic states or hot spots were also included based on prior knowledge (*TP53* allelic state, *IDH2* hot spots) or univariate comutation analysis (*TET2* allelic state, *U2AF1* hot spots). (B) Rules of co-occurrence and mutual exclusivity of genetic alterations organized in a hierarchical classification tree.

clinical profile including elevated blasts and increased risk of leukemic transformation yet no excess risk of death.²⁷

The *AML-like* group (2%, $n = 66$; supplemental Figure 14) was defined by *NPM1* mutations ($n = 39$), *inv(3)/t(3;3)* ($n = 8$), or at least 2 events from *WT1*, *FLT3*, *MLL*^{PTD}, or *MYC* mutations ($n = 22$). Of the 8 cases with *inv(3)/t(3;3)*, 5 had a *SF3B1* mutation (VAF, 5%-36%). The *AML-like* group showed the highest percentage of BM blast (median, 10% vs 3%; $P < .0001$;

supplemental Figure 9). It was also associated with a younger age (median, 65 vs 72 years; $P < .0001$), a female predominance (53% vs 39%; OR, 1.7; $P = .03$), short OS (median, 0.9 years [interquartile range [IQR]; 0.5-2.3]), and had the highest rate of leukemic transformation (40% vs 14% for other MDS at 2 years; Figure 4B). Those associations were preserved when separating patients with established AML-defining *NPM1* mutations or *inv(3)* vs other AML-like mutations (supplemental Figure 14).

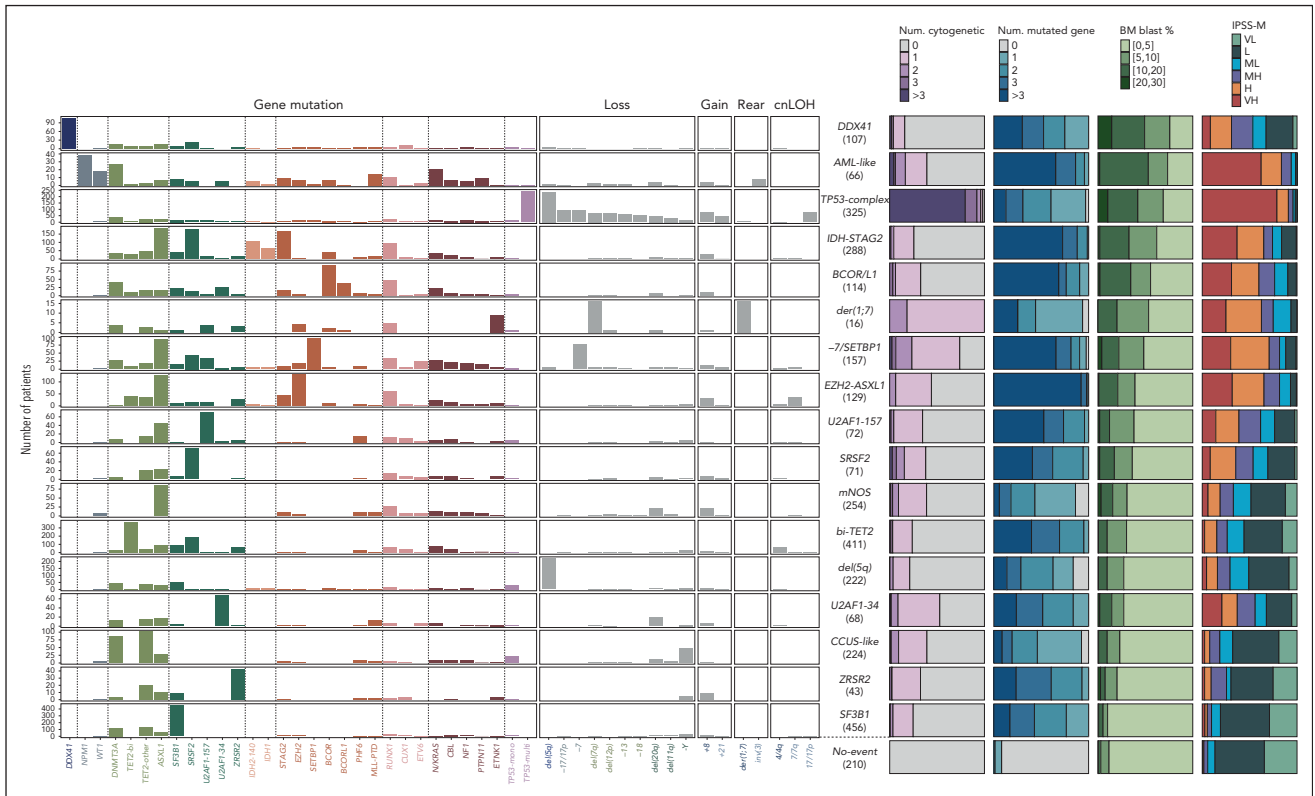


Figure 3. Molecular composition and main characteristics of MDS molecular groups. Each row represents a molecular subgroup, and molecular features are ordered by blocks of gene mutations, chromosomal losses, gains, rearrangements, and cnLOH events. For each subgroup, the relative proportions of (1) the number of mutated genes per patient, (2) the number of cytogenetic alterations per patients, (3) the proportion of BM blasts, and (4) IPSS-M risk category are indicated as stacked bar plots. H, high; L, low; MH, moderate high; ML, moderate low; VH, very high; VL, very low.

Multihit *TP53* alterations have been incorporated in the WHO 2022/ICC MDS-bi*TP53* entity.^{9,10} In the *TP53-complex* group (10%, n = 325; supplemental Figure 15), multihit *TP53* mutations were present in 241 (74%) cases, of which 219 (91%) had CK. Only 13 cases (4%) had monoallelic *TP53* mutations and CK. Among the 303 (93%) cases with CK, 71 (23%) had no detected *TP53* mutation. This allowed us to compare CK cases with (n = 232) or without (n = 71) *TP53* mutation (supplemental Figure 18). As expected,²⁸ CK cases with *TP53* mutations (CK:*TP53*) had more cytogenetic abnormalities compared with those with CK only (73% vs 20% with ≥ 6 events; OR, 10.8; $P < .0001$); deletion of 5q occurred in 87% and 32%, respectively. Only trisomy 8 and deletion of 11q were more frequent in the CK-only group. The CK-only subset had more mutated genes than the CK:*TP53* group (46% vs 24% with ≥ 3 mutated genes; OR, 2.8; $P = .0005$), with enrichment for *RUNX1*, *SRSF2*, and *SF3B1* mutations. OS was poor in both CK subsets, albeit shorter in the presence of *TP53* mutation (median, 0.7 vs 1.5 years; $P < .0001$; supplemental Figure 18). Therefore, although our categorization did not formally distinguish between CK with or without *TP53* mutation, differences in molecular profiles and outcomes support a sub-categorization, as suggested by Huber et al.²⁶

The *del(5q)* group (6.9%, n = 222; supplemental Figure 16) was defined by the presence of *del(5q)* as the sole cytogenetic abnormality or with 1 additional abnormality excluding $-7/7q$.^{9,10,29} In this group, 84% of patients had at least 1 gene mutation, most commonly *SF3B1* (22%), *DTA* (*DNMT3A*, *TET2*,

ASXL1: 21%, 17%, 14%), and monoallelic *TP53* (13%) mutations. Monoallelic *TP53* mutations were significantly enriched in this group (OR, 4.8; $P < .0001$), along with mutations in *CSNK1A1* (10%; OR, 16.4; $P < .0001$), *IRF1* (5.4%; OR, 19.0; $P < .0001$), and *RAD50* (4.1%; OR, 14.1; $P < .0001$), all located on 5q, and *NFE2* (3.6%; OR, 5.1; $P = .0006$). Gene mutations occurred secondary to *del(5q)* (supplemental Figure 19).³⁰ *Del(5q)* was associated with a female bias (75% vs 37%; $P < .0001$), low hemoglobin values, high platelet counts, and favorable OS (Figure 4B). Notably, 22% (49/222) of cases from our *del(5q)* group would be excluded from the WHO 2022/ICC MDS with isolated *del(5q)* category because of excess blasts. Only 1% of cases were CMML per WHO 2016 compared with 8% per the new WHO 2022 definition of CMML.

The *SF3B1* group (14%, n = 456; supplemental Figure 17) was the most prevalent. Comutations were relatively infrequent, with 23% of cases having isolated *SF3B1* mutations, and 27% of cases having only *SF3B1* and *DTA* mutations.^{31,32} *SF3B1* mutations were frequently secondary to *DNMT3A* mutations and dominant to *TET2* mutations. The group had low BM blasts (median, 1.5% [IQR, 1-3]) and favorable outcomes (median OS, 6 years [IQR, 3-12]). Per WHO 2016, 80% of cases had low-blast MDS, 8% had excess blasts, and 12% had MDS/MPN. Per WHO 2022 and ICC, 60% and 54% of cases were MDS-*SF3B1*, respectively (25 discordant cases classified as MDS-NOS per ICC, with *SF3B1* VAF of $<10\%$ or *RUNX1* mutations). Of 355 cases with low-blast MDS, 85 (24%) met monocyte criteria for CMML per WHO 2022.

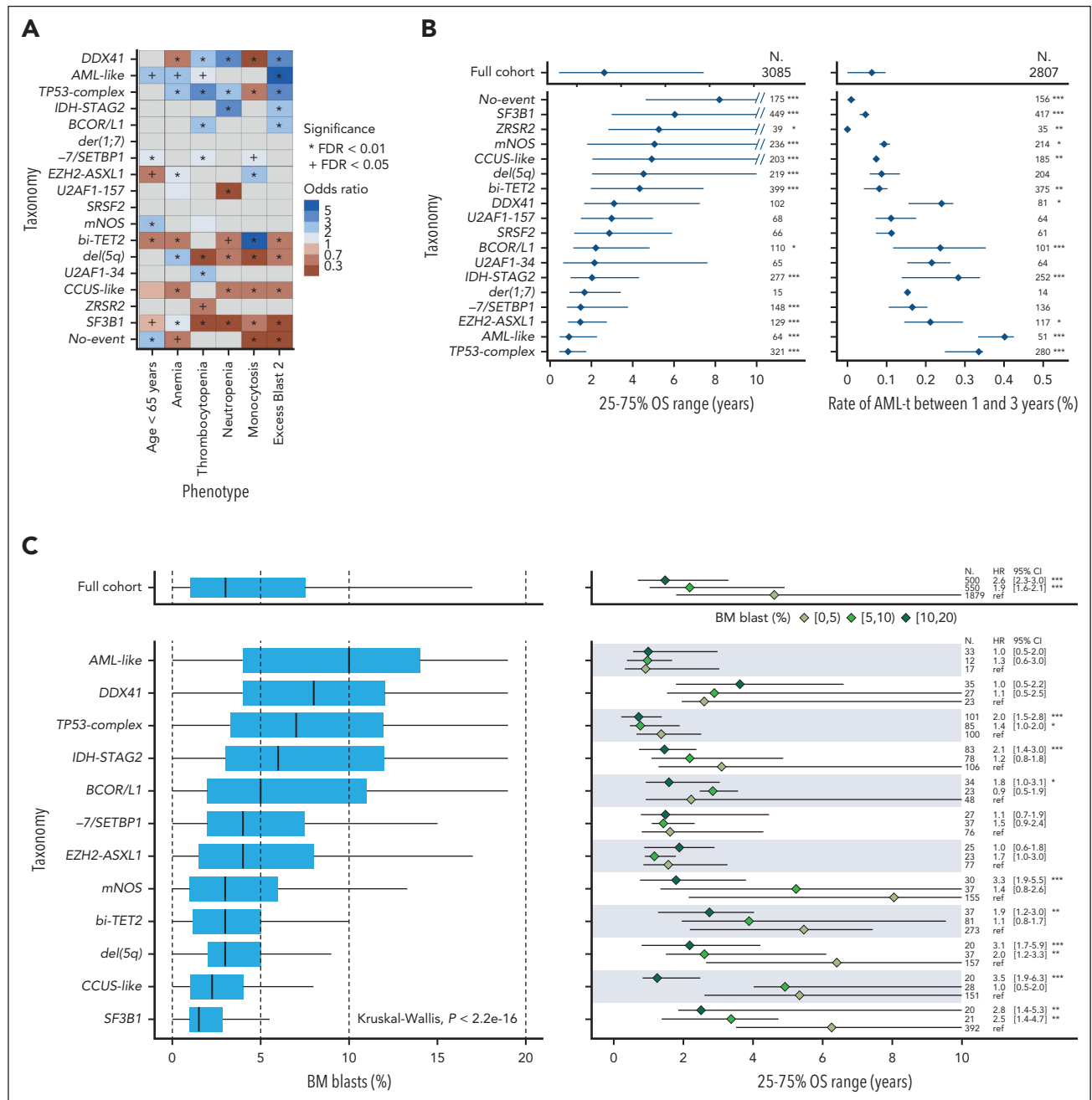


Figure 4. Associations between MDS molecular groups, clinical phenotypes, and outcomes. (A) Association between molecular groups and clinical phenotypes. Darker blue indicates co-occurrence, and darker red indicates mutual exclusivity. (B) Association between molecular groups and outcomes, for OS (left) and AML transformation (AML-t, right). Dots indicate median OS and lines extend to the interquartile range (left). Dots indicate the 2-year incidence of AML-t and lines extend to the 1-year and 3-year incidences (right). The outcome metrics on the full cohort are provided on top for comparison. *P* values are from the log-rank test (OS) and the Gray test (AML-t). ****P* < .001; ***P* < .01; **P* < .05. (C) Distribution of the percentage of BM blast for 12 molecular groups with at least 10 patients within each subset of BM blast, that is, 0% to 5%, 5% to 10%, and 10% to 20% (left). Median survival (dots) and interquartile range (lines) for each blast subset within each molecular group (right). *P* values are from a univariate Cox model with the 0% to 5% blast subset used as the reference level. The distributions of the full cohort are provided on top for comparison. (D) Cumulative incidence curves of AML-t stratified with the range of percentage of BM blast within the *DDX41* and *AML-like* subgroups. *P* values are from the Gray test. (E) Kaplan-Meier probability estimates of OS stratified with the range of percentage of BM blast within the *EZH2-ASXL1* and *-7/SETBP1* subgroups. *P* values are from the log-rank test. CI, confidence interval; HR, hazard ratio; ref, reference level.

Previously reported subsets: *bi-TET2*, *der(1;7)*, and *CCUS-like*

The second largest group was defined by biallelic *TET2* mutations (13%, *n* = 411; supplemental Figure 20), which has been recognized in few studies despite its prevalence.^{21,33} Patients in this group had distinct clinicohematological features, including

older age, milder anemia, increased monocytes, and a CMML enrichment (42%; Figure 4A).

The *bi-TET2* group was defined by early biallelic *TET2* mutations with splicing factor mutations in 80% of patients, most commonly affecting *SRSF2*, *SF3B1*, or *ZRSR2* (185/411, 86/411,

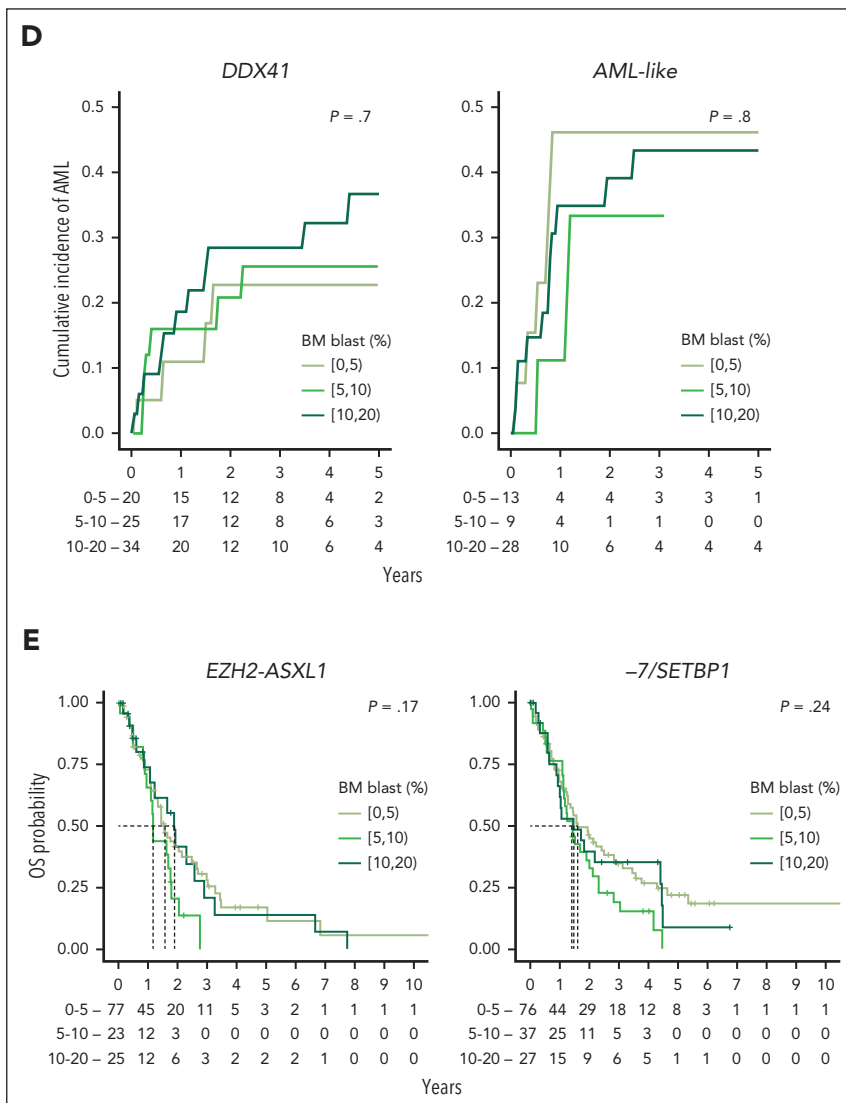


Figure 4 (continued)

and 65/411, respectively; supplemental Figures 20-21). The association with elevated monocytes within *bi-TET2* was preserved across all splicing factor mutation subsets. However, comutations further modulated the phenotypes: in multivariable analysis, *SF3B1* and *JAK2* mutations were both predictors of higher platelet count, whereas *SF3B1* mutations were predictive of lower hemoglobin level. *RUNX1* mutations were predictive of higher blasts, and *ASXL1* and *RAS* pathway mutations of higher WBC and monocyte counts (supplemental Figure 21). Although secondary events influenced the overall disease phenotype, all molecular trajectories converged on a bias toward monocytic differentiation.

The *der(1;7)* group (0.5%, $n = 16$) was a rare subset characterized by *der(1;7)(q10;p10)*, previously reported to be enriched in Japanese populations.^{34,35} There was a male predominance (14/16) and a relatively young age (median, 64 years [IQR, 55-70]). *ETNK1* mutations were enriched in this group (56%; OR, 61; $P < .0001$) as secondary events (median VAF, 25%).

In the *CCUS-like* group (6.9%, $n = 224$; supplemental Figure 22), 104 (46%) patients had a single mutated gene (45 *TET2*, and 37 *DNMT3A*), 17 (8%) had loss of Y without gene mutations, and 14 (6%) only had ≥ 2 *DTA* mutations. *CCUS-like* had low cancer cell fractions compared with other groups (median, 42% vs 84%; $P < .0001$), reflecting smaller clonal cytopenia of unknown significance (*CCUS*) clone sizes.³⁶ The group was associated with lower risk (68% *IPSS-M* very low/low) and favorable outcomes (median OS, 4.9 years [IQR, 2 to not reached]).

Novel molecular groups: -7/SETBP1, EZH2-ASXL1, IDH-STAG2, BCOR/L1, U2AF1¹⁵⁷, U2AF1³⁴, SRSF2, and ZRSR2

The -7/*SETBP1* group (4.9%, $n = 157$; supplemental Figure 23) was defined by *SETBP1* mutations and/or -7 in the absence of *CK* (OR, 9; $P < .0001$).^{37,38} Within this group, 11% of patients had both *SETBP1* mutation and -7, 51% only *SETBP1* mutation, and 38% only -7. *SETBP1* mutations were secondary events (median VAF, 24%). Clonally dominant events included *ASXL1*,

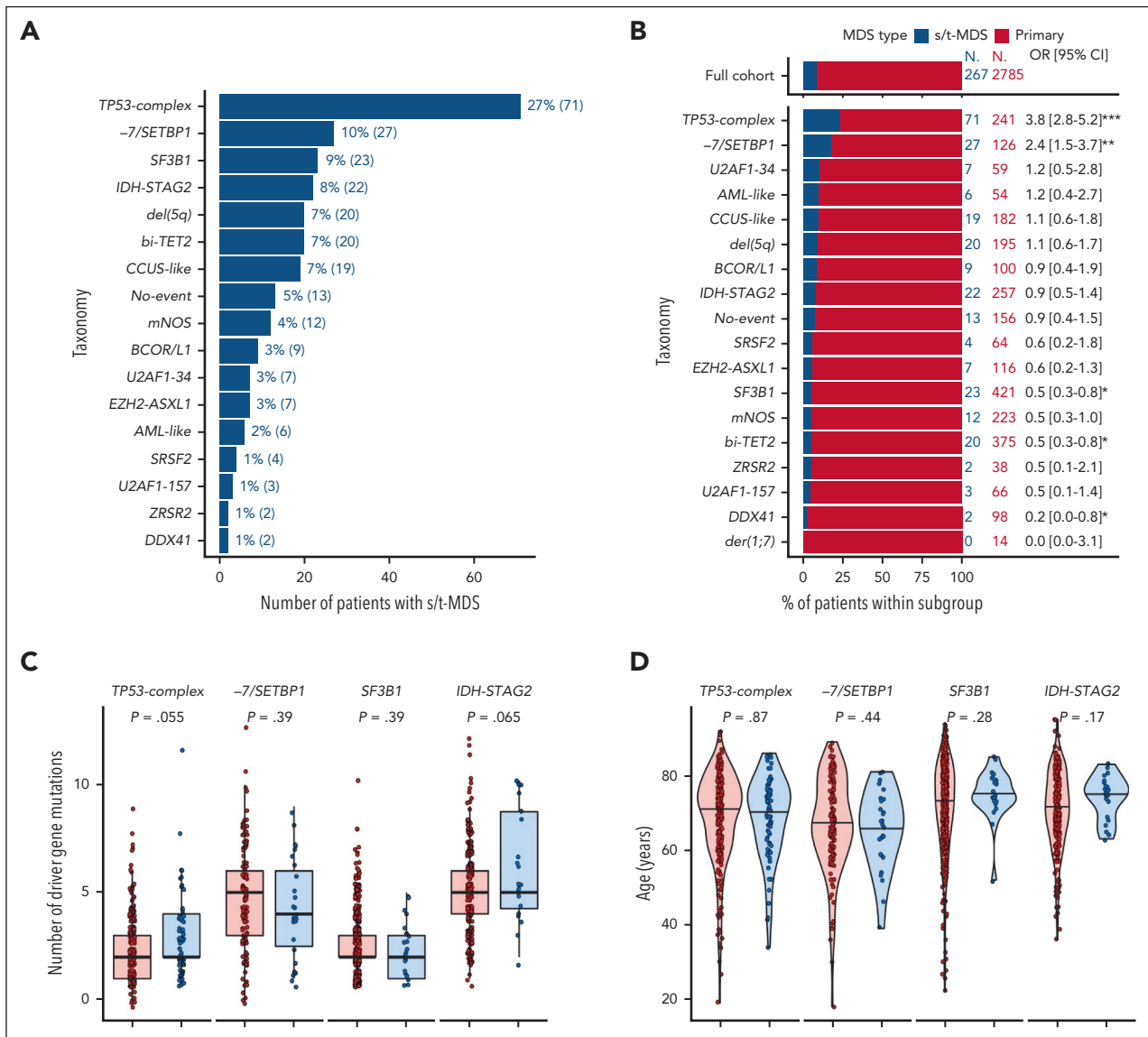


Figure 5. Genetic heterogeneity of s/t-MDS. (A) Prevalence of molecular groups in 267 patients with s/t-MDS. (B) Proportion of primary (red) and s/t-MDS (blue) within each molecular group and comparison with the full cohort (top). (C) Distribution of the number of mutated driver genes per patient in primary or s/t-MDS within each molecular group (*TP53-complex*, *-7/SETBP1*, *SF3B1*, and *IDH-STAG2*), showing similar molecular complexity of the 2 disease subsets. For example, the median number of mutated genes per patient was equal to 2 for both primary and s/t-MDS within *TP53-complex*, whereas it was equal to 5 for both subsets within *IDH-STAG2*. (D) Age distribution in primary or s/t-MDS within each molecular group. (E) Kaplan-Meier probability estimates of OS for primary or s/t-MDS within each molecular group. *P* values are from the log-rank test.

SRSF2 (enriched in the *SETBP1*-only subset), or *U2AF1* Q157 mutations. *GATA2* mutations were also overrepresented (OR, 6.8; *P* < .0001), with VAFs suggestive of germ line variants in 6 (4%) patients (median age, 59 years; range, 18-80).³⁹ The *-7/SETBP1* group was associated with a younger age (median, 67 vs 72 years; *P* < .0001), particularly for the subset with both *SETBP1* mutation and *-7* (median, 61 years [IQR, 56-69]). The sequencing panel excluded *SAMD9/L* genes linked to germ line driven *-7* reversion in MDS.⁴⁰ Further research is needed to investigate *SAMD9/L* or other germ line variants in the *-7/SETBP1* group. Last, *-7/SETBP1* was characterized by higher risk (71% IPSS-M very high/high) and poor outcomes (median OS, 1.5 years [IQR, 0.8-3.8]).

The *EZH2-ASXL1* group (4%, *n* = 129; supplemental Figure 24) was defined by *ASXL1* and *EZH2* mutation co-occurrence. It was

characterized by a high molecular complexity (75% of patients with ≥ 5 mutated genes). Half of cases had splicing factor mutations in *ZRSR2* (20% [26/129]), *U2AF1* Q157 (12%), *SRSF2* (11%), and *SF3B1* (8%). *EZH2* mutations were frequently subclonal to *TET2*, *ASXL1*, and splicing factor mutations. This group had the highest proportion (47%) of secondary *RUNX1* mutations. Although 60% of cases had BM blasts of <5%, this group was associated with poor OS (median, 1.5 years [IQR, 0.9-2.8]). Splicing factor mutations in this context were not associated with differing survival or comutation patterns (supplemental Figure 25).

The *IDH-STAG2* group (8.9%, *n* = 288; supplemental Figure 26) was defined by mutations at the *IDH2* R140 hot spot, *IDH1*, and/or *STAG2* co-occurring with either *SRSF2* or *ASXL1* mutations. Mutations in *IDH2*, *SRSF2*, and *ASXL1* were generally

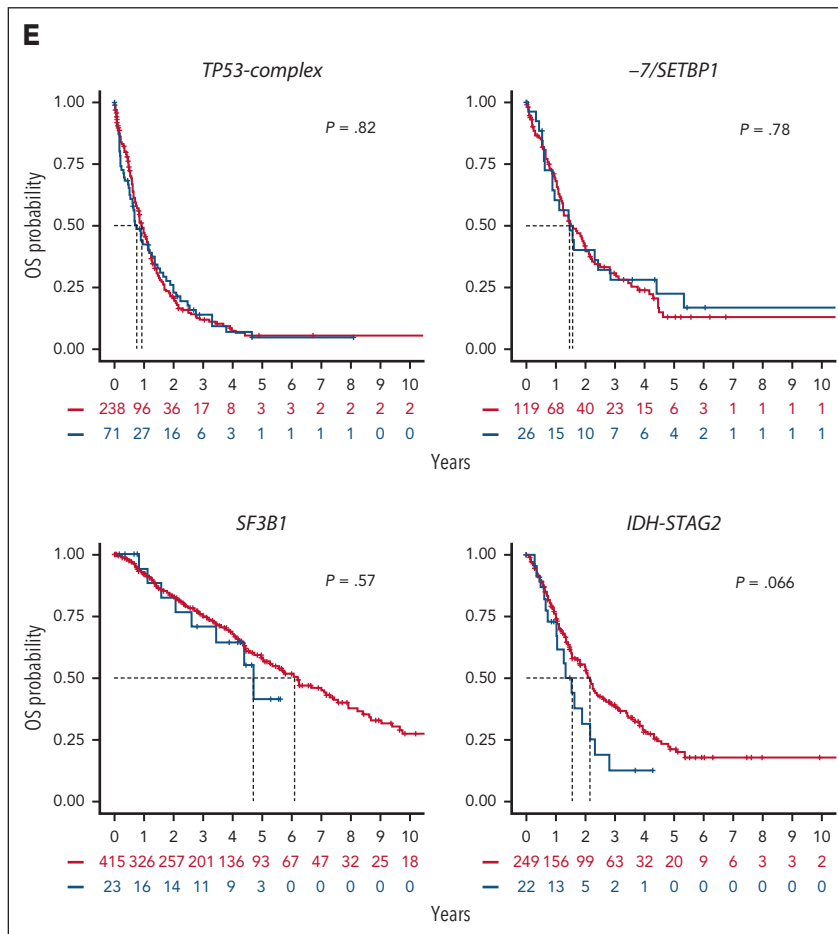


Figure 5 (continued)

acquired early whereas *STAG2* mutations were late. The composite genotypes of this group mirrored secondary AML,^{41,42} and the myelodysplasia-related AML (WHO²⁰²²) or AML with MDS-related gene mutations (ICC) subtypes.^{43,44} Accordingly, this group had elevated BM blasts (median, 6% [IQR, 3-12]; supplemental Figure 9). Median BM blasts of cases with both *IDH1/2* and *STAG2* mutations, *STAG2* only, and *IDH1/2* only were 12% (IQR, 7-15), 8% (IQR, 4-13), and 4% (IQR, 2-8), respectively. This group had the third highest 2-year incidence rate of AML transformation (28%) after *AML-like* and *TP53-complex* (Figure 4B).

In the *BCOR/L1* group (3.5%, n = 114; supplemental Figure 27), 83% of patients had mutations in *BCOR*, 33% in *BCORL1*, and 17% in both genes. *BCOR/L1* mutations were secondary to *DTA* and splicing factor mutations. The latter occurred in 61% of patients: *U2AF1* S34 mutations were most frequent (22%; OR, 9.4; $P < .0001$), followed by *SF3B1* (21%) and *SRSF2* (11%) mutations. Subclonal *RUNX1* mutations were frequent (41%). *BCOR/L1* was characterized by pronounced thrombocytopenia, elevated BM blasts, short OS (median, 2.2 years [IQR, 1.1-4.8]), and a 24% 2-year incidence of AML transformation. These phenotypic associations were irrespective of splicing factor mutation status (supplemental Figure 28).

The last 4 groups, *U2AF1*¹⁵⁷ (2.2%, n = 72), *U2AF1*³⁴ (2.1%, n = 68), *SRSF2* (2.2%, n = 71), and *ZRSR2* (1.3%, n = 43), were defined based on the exclusion of the aforementioned group-defining events and the residual presence of distinct splicing factor mutations other than *SF3B1*. Patients from these groups had fewer mutations, with 38% (96/254) having only 1 or 2 mutated genes (Figure 3). The *ZRSR2* group, specific to males, correlated with indolent clinical phenotypes and favorable OS (median, 5.3 years [IQR, 3.5 to not reached]; Figure 4A-B).

Residual groups: *mNOS* and *No-event*

The last 2 groups were defined by negative findings: *mNOS* (absence of group-defining patterns) and *No-event* (absence of recurrent mutations or cytogenetic). Both groups were associated with mild phenotypes and favorable outcomes (Figure 4A-B). Compared with cases with oncogenic events, patients without identified drivers were younger (median age, 65 vs 72 years; $P < .001$), with a female bias (61% vs 38%; OR, 2.5; $P < .001$), frequent classification as MDS with single-/multilineage dysplasia (73% vs 27%; OR, 7.1; $P < .001$), lower risk IPSS-M (75% vs 36% as very low/low; OR, 5.5; $P < .001$), and favorable OS (median, 7.6 vs 3.0 years; $P < .001$; supplemental Figure 29). A concomitant study demonstrated that the male subset of the *No-event* group was enriched for *UBA1* mutations (7%) and VEXAS-like clinical presentation.⁴⁵

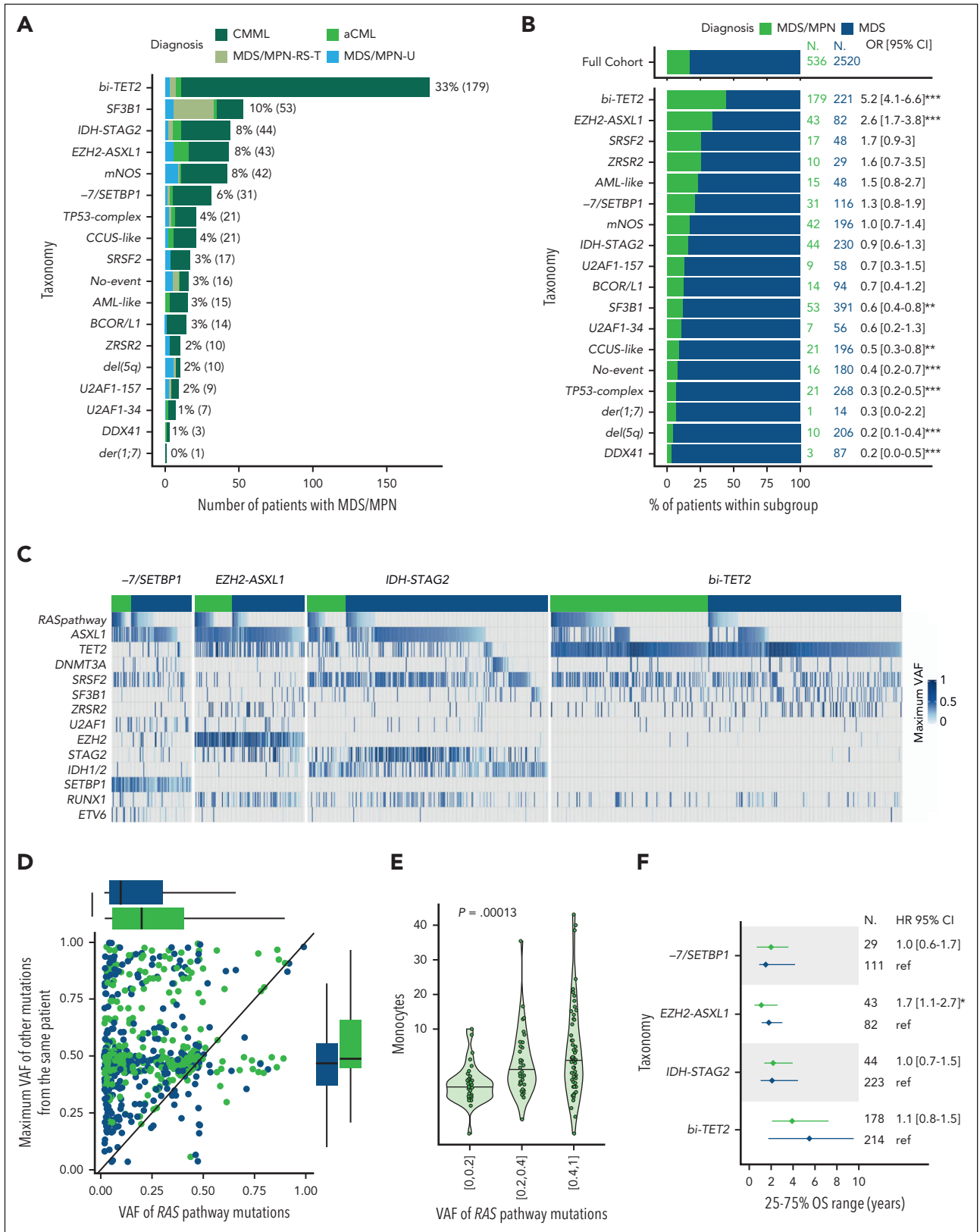


Figure 6. Genetic heterogeneity of MDS/MPN with ubiquitous RAS pathway mutations enrichment. (A) Prevalence of molecular groups in 536 patients with MDS/MPN color-coded by specific subtypes. The *bi-TET2* group accounted for 33% of MDS/MPN cases and 42% (168/399) of CMML cases. The *EZH2-ASXL1* group comprised 8% of MDS/MPN cases and 26% (10/38) of atypical chronic myeloid leukemia (aCML) cases. The majority of MDS/MPN with ring sideroblasts and thrombocytosis (MDS/MPN-RS-T) cases (63%, 27/43) were part of the *SF3B1* group. (B) Proportion of MDS/MPN (green) and MDS (blue) within each molecular group and comparison with the full cohort (top). (C) Oncoplots for each molecular group (*-7/SETBP1*, *EZH2-ASXL1*, *IDH-STAG2*, and *bi-TET2*) separating MDS/MPN (green) and MDS (blue). Each column corresponds to a patient. The presence of a mutation in each gene for each patient is color-coded by the VAF (maximum VAF if several mutations within the same gene). RAS pathway

Nonetheless, 11% (21/193) of cases without identified drivers had excess blasts (median BM blasts, 7% [range, 5%-15%]). We therefore performed whole-genome sequencing from 30 patients with excess blasts that did not have an identified driver ($n = 20$) or only had $-Y$ or DTA mutation ($n = 10$; $-Y$ in 1, $DNMT3A$ in 4, $TET2$ in 4, and $ASXL1$ in 1). We identified additional putative oncogenic events in 27% (8/30) of cases. This included 1 $NUP98-MLL$ fusion, chromosome 20 and 22 abnormalities, and 1 $UBA1$ M41T mutation in a male patient (5% BM blasts), and possibly germ line frameshift mutations in ATR , $FANCC$, $INPPL1$, and $RTEL1$ (supplemental Table 7).

The prognostic influence of BM blasts within genetic subtypes

Blast count thresholds (<5% for low blast, 5%-9% for excess blasts 1, and 10%-19% for excess blasts 2) are defining features in MDS classifications.⁸⁻¹⁰ We evaluated how genetic subtypes relate to BM blast strata. In our data set, 61% (1974) of patients had <5% blasts, 18% (566) had 5% to 9%, and 16% (507) had 10% to 19%.

Seven to 9 different molecular groups accounted for >5% of patients within each blast stratum (supplemental Figure 30). This molecular heterogeneity translated into variability in outcomes, whereby the OS of patients within each blast stratum stratified with the molecular groups. However, contrary to prior findings,²⁶ both molecular groups and blast percentages were independently predictive of OS (supplemental Figure 30). We reasoned that the impact of BM blast counts on outcomes might depend on the specific molecular subtype, and we therefore investigated the effect of blast counts on the OS of patients within each molecular group.

We focused on the 12 groups with at least 10 patients with outcome data per blast stratum (Figure 4C; supplemental Figure 31). In 8 groups ($SF3B1$, $CCUS$ -like, $del(5q)$, $bi-TET2$, $mNOS$, $BCOR/L1$, $IDH-STAG2$, and $TP53$ -complex), blast count differentiated OS. Of note, blast stratification was significant in the $TP53$ -complex group but outcomes were all very poor (median OS: 1.4, 0.8, and 0.7 years across the 3 strata; supplemental Figure 32). For 4 groups ($EZH2-ASXL1$, $-7/SETBP1$, $DDX41$, and AML -like), OS was not stratified by blast count. $DDX41$ and AML -like had the highest blasts of all groups: 49% (51/104) and 53% (34/64) of patients had $\geq 10\%$ blasts, respectively. Yet, within the $DDX41$ and AML -like groups, both the OS and the rate of leukemic transformation were comparable across the 3 blast strata (Figure 4D; supplemental Figure 31). This effect in AML -like was independent of $NPM1$ mutations (supplemental Figure 32). Conversely, the $EZH2-ASXL1$ and $-7/SETBP1$ groups were enriched for low blasts, with 61% (77/126) and 52% (79/152) of patients having <5% blasts, respectively. However, the OS of patients in those 2 groups was poor independently of blasts (median OS, <2 years in each stratum; Figure 4E). This demonstrates that specific

genetic subtype outweighs blast count as a predictor of outcomes, which should be considered in a future MDS classification.

Genetic heterogeneity of s/t-MDS

We used the molecular groups to investigate genetic heterogeneity in s/t-MDS. We first evaluated the repartition of 267 patients with s/t-MDS across molecular groups (Figures 5A-B). As expected, the $TP53$ -complex group was the most frequent within s/t-MDS (27%) and enriched in this subset compared with primary MDS (OR, 3.8; $P < .001$).⁴⁶⁻⁴⁸ The remaining 73% of patients with s/t-MDS spread across 16 other groups, predominantly $-7/SETBP1$ (10%, 27/267), $SF3B1$ (9%), and $IDH-STAG2$ (8%). The $-7/SETBP1$ group was enriched in s/t-MDS (OR, 2.4; $P < .01$), whereas the $SF3B1$, $bi-TET2$, and $DDX41$ groups were underrepresented (OR: 0.5, 0.5, and 0.2, respectively; $P < .05$).

When selecting groups with >20 patients with s/t-MDS ($TP53$ -complex, $-7/SETBP1$, $SF3B1$, and $IDH-STAG2$), and comparing s/t-MDS with primary MDS, we observed similar molecular (Figure 5C; supplemental Figure 33), clinical (Figure 5D; supplemental Figure 34), and outcome (Figure 5E) profiles. The younger age characterizing $-7/SETBP1$ was conserved in s/t-MDS (median age, 67 years; range, 39-81). We, and others, have shown that the IPSS-M efficiently risk stratifies patients with s/t-MDS.^{3,49} Here, we demonstrated that the heterogeneity in outcomes within s/t-MDS can be partially explained by the underlying molecular subtypes. Indeed, the median OS of patients with s/t-MDS across $TP53$ -complex, $-7/SETBP1$, $IDH-STAG2$, and $SF3B1$ groups were 0.8, 1.5, 1.6, and 4.7 years, respectively, which was similar to the OS of the respective primary MDS subsets (Figure 5E).

Genetic heterogeneity of MDS/MPN with ubiquitous RAS pathway mutations enrichment

The distribution of molecular subgroups in 536 patients with MDS/MPN (WHO 2016) was heterogeneous and consistent with prior studies (Figure 6A).⁵⁰ Fifteen groups were observed in >1% of patients, and 6 groups ($bi-TET2$, $SF3B1$, $IDH-STAG2$, $EZH2-ASXL1$, $mNOS$, and $-7/SETBP1$) in >5% of patients. Among those, $bi-TET2$ and $EZH2-ASXL1$ were enriched in MDS/MPN compared with MDS (OR, 5.2 and 2.6, respectively; $P < .0001$; Figure 6B). Beyond the genes defining the enriched groups ($TET2$, $EZH2$, $ASXL1$, and $SRSF2$), RAS signaling pathway mutations (OR, 4.8; $P < .0001$) and, to a lesser extent, $RUNX1$ mutations (OR, 1.4; $P < .01$) were enriched in MDS/MPN. RAS pathway mutations were consistently overrepresented in MDS/MPN across the $-7/SETBP1$, $EZH2-ASXL1$, $IDH-STAG2$, and $bi-TET2$ groups (Figure 6C; supplemental Figure 35). Moreover, the VAF of RAS pathway mutations was higher in MDS/MPN (median, 20% [IQR, 6-42]) than in MDS (median, 10% [IQR, 4-31]; $P < .0001$) across molecular subgroups (Figure 6C-D; supplemental Figure 35).

Figure 6 (continued) mutations include mutations in $N/KRAS$, CBL , $NF1$, and $PTPN11$. They were observed in 68%, 51%, 45%, and 40% of patients with MDS/MPN within groups $-7/SETBP1$, $EZH2-ASXL1$, $IDH-STAG2$, and $bi-TET2$, respectively, compared with 33%, 21%, 14%, and 15% of patients with MDS within the same groups. (D) Scatterplot representing 1 dot per patients with RAS pathway mutation, with the VAF of RAS pathway mutations on the x-axis and the maximum VAF of all other mutations in the same patient on the y-axis. (E) Monocyte level in $10^9/L$ as a function of the VAF of RAS pathway mutations in the subset of 297 patients with MDS/MPN from the same molecular groups as in panel C. (F) Median survival (dots) and interquartile range (lines) for MDS/MPN (green) and MDS (blue) within each molecular group. Patients from the $bi-TET2$ group had favorable OS (median, 5.5 and 3.9 years for MDS and MDS/MPN, respectively). Conversely, patients from the $IDH-STAG2$, $EZH2-ASXL1$, and $-7/SETBP1$ groups had dismal OS in both subsets (median, 2.1, 1.8, and 1.5 years, respectively, in MDS and 2.2, 1.1, and 2.0 years, respectively, in MDS/MPN).

We explored molecular predictors of WBC and monocyte levels. In multivariable regressions for leukocytosis and monocytosis, the presence of *RAS* pathway, *SRSF2*, biallelic *TET2* (but not monoallelic), and *ASXL1* mutations were positive predictors for both parameters (supplemental Figure 36). *EZH2* mutations predicted for leukocytosis but not monocytosis, consistent with the atypical CML enrichment in the *EZH2-ASXL1* group (OR, 8.8; $P < .001$). The 185 patients with MDS from the *bi-TET2* group had higher monocyte counts than the 1675 patients with MDS from other groups (48% vs 24% with $\geq 0.5 \times 10^9/L$; supplemental Figure 37). In addition, the VAF of *RAS* pathway mutations strongly predicted increased monocyte counts in multivariable analysis (Figure 6E; supplemental Figure 36).^{51,52} This effect was stronger in MDS/MPN than MDS (supplemental Figures 36-37), suggesting that considerable expansion of *RAS* pathway mutated clones is necessary to drive elevated monocyte counts at diagnosis.

Last, we compared the clinical phenotypes and outcomes of patients categorized as MDS or MDS/MPN within molecular groups. Despite expected differences in WBC and monocyte counts, age, blast, hemoglobin, and platelet distributions were comparable within each group (supplemental Figure 38), as well as OS (Figure 6F; supplemental Figure 39). Thus, similar to our observations in s/t-MDS, the genetic subtype plays a dominant role in the overall clinical phenotype (aside from the MDS/MPN-defining features of WBC and monocyte counts) and outcomes irrespective of morphologic classification as MDS or MDS/MPN.

Discussion

Diagnostic classification of hematologic neoplasms rely predominantly on morphological features, which do not adequately account for heterogeneous clinical phenotypes and outcomes. Deletion 5q, *SF3B1*, and biallelic *TP53* mutations are established subtype-defining MDS biomarkers.^{9,10} However, the majority of genetic lesions are not yet considered. A broader integration of genetic alterations will improve our understanding of disease ontogeny; the design of clinical trials; and, ultimately, the diagnosis and treatment of MDS.

We characterized 18 MDS subtypes (16 genetic groups and 2 residual groups) each associated with specific clinical phenotypes and disease courses. The subtypes were defined by combinations of chromosomal aneuploidies, cnLOH events (*TP53* and *TET2* loci), gene mutations, and gene-gene interactions. We validated established (*TP53-complex*, *del(5q)*, and *SF3B1*) or well-characterized entities (*DDX41* and *AML-like*), substantiated support for emerging subtypes (*bi-TET2*, *der(1;7)*, and *CCUS-like*), and unveiled novel groups (*-7/SETBP1*, *EZH2-ASXL1*, *IDH-STAG2*, *BCOR/L1*, *U2AF*¹⁵⁷, *U2AF*¹³⁴, *SRSF2*, and *ZRSR2*). Unlike published MDS genetic hierarchies,⁵ splicing factor mutations were not at the top of the classification tree. For several subgroups, the defining events were secondary to DTA and/or splicing factor mutations (*SETBP1*, *EZH2*, *STAG2*, or *BCOR/L1* mutations), reminiscent to *NPM1* mutations defining a unique AML subtype while often being secondary to *DNMT3A* mutations.⁵³ Study limitations included the use of targeted sequencing, which might have omitted pertinent

biomarkers (eg, *SAMD9/L* variants and *UBTF* tandem duplication), the absence of germ line control tissues, and the lack of correlative analysis with some relevant morphological features, such as cellularity and fibrosis.

We evaluated the relationship between genetic subtypes and blasts. In several groups (*AML-like*, *DDX41*, *-7/SETBP1*, and *EZH2-ASXL1*), blast percentages did not stratify patient outcomes. However, for groups enriched for lower-risk disease (for example *del(5q)*, *bi-TET2*, *SF3B1*, *CCUS-like*, and *mNOS*) blast percentages differentiated outcomes. This suggests a novel paradigm in which the genetic subtypes should be the overarching basis of disease classification, whereby blasts designate disease stage within certain genetic contexts, for example *del(5q)* or *IDH-STAG2* with increased blasts, as Kewan et al also have suggested.⁶

These molecular subgroups facilitated the evaluation of genetic heterogeneity in s/t-MDS and MDS/MPN. Although enriched in specific subtypes (*TP53-complex* and *-7/SETBP1*), s/t-MDS were represented across most genetic groups, including those associated with favorable outcomes (*SF3B1*). This suggests that although some chemotherapy-resistant molecular subtypes are promoted by prior therapy,⁵⁴ others may arise from other mechanisms. Patients with s/t-MDS and primary MDS had comparable clinical profiles and outcomes within genetic subtypes. MDS/MPN were also represented across diverse genetic subgroups (*SF3B1*, *IDH-STAG2*, and *EZH2-ASXL1*) but were strongly enriched in the *bi-TET2* group, which was associated with elevated monocytes across disease categories. A higher frequency and clonal expansion of *RAS* pathway mutations in MDS/MPN over MDS was ubiquitous across genetic subtypes. This argues for the recognition of *bi-TET2* as a unique entity encompassing both MDS and MDS/MPN, and for the prospective monitoring of *RAS* pathway mutations as potential biomarkers predictive of monocytic proliferation.

The molecular taxonomy outlined in this study identifies groups of patients with MDS with shared molecular pathogenesis, providing the foundation for a broader genetically informed classification of MDS. Its purpose is different from that of prognostic assessments, such as IPSS-M, whereas both inform clinical decision-making. Prognostic schemas consider clinical and molecular features to estimate patient outcomes, thus guiding risk-adapted therapies. However, there is no equivalence between risk and molecular groups: 2 patients from the *TP53-complex* or *EZH2-ASXL1* molecular groups may both be categorized as high risk although distinct. The definition of molecular groups is key to identifying determinants of disease progression and treatment response. This molecular taxonomy should be a useful tool for future correlative studies and exploratory analyses within clinical trials evaluating the efficacy of therapeutic compounds and for the development of targeted therapies.

Acknowledgments

This work was supported in part by grants from Celgene Corporation through the MDS Foundation. E.B. was supported by the Edward P. Evans Foundation and the INSERM ATIP-Avenir Program. L.M. was supported by the Associazione Italiana per la Ricerca sul Cancro (AIRC), Milan, Italy (investigator grant 20125; AIRC 5×1000 project 21267);

Cancer Research UK, Fundación Científica de la Asociación Española Contra el Cáncer's (FC AECC) and AIRC-International Accelerator Award Program (project C355/A26819 and 22796). V.S. was supported by AIRC project IG-26537. L.-Y.S. was supported by MOHW111-TDU-B-221-01400. U.G. and N.G. were supported by the Deutsche Krebshilfe grant 70113711. M.G.D.P. was supported by AIRC project 22053 and AIRC 5×1000 project 21267. M.Y.F. was supported by Italian MIUR-PRIN (grant 2017RKWNJT) and the Fondazione Carisbo. E.P. was supported by the Josie Robertson Investigators Program.

Authorship

Contribution: E.B. and E.P. designed the study, analyzed the data, and wrote the paper; E.B. created the figures; E.B., J.E.A.O., J.G.-A., D.D., J.S.M.-M., M.L., K.L., and N.F. executed bioinformatics pipelines; R.P.H., P.L.G., H.T., B.L.E., R.B., L.M., M. Cazzola, M. Creignou, S.O., and E.H.-L. critically reviewed the data; R.P.H. reviewed established classification of all included cases; L.M., F.P.S.S., M. Creignou, U.G., A.A.v.d.L., M.J., M.T., O.K., M.Y.F., F.T., R.F.P., V.S., I.K., J.B., F.P.S.S., V.M.K., M.R.S., M.B., C.G., L.P., L.A., M.G.D.P., P.F., A.P., U.P., M.H., P.V., C.F., M.T.V., L.-Y.S., M.F., J.H.J., J.C., N.G., M. Cazzola, and E.H.-L. provided clinical data and DNA specimens; and all authors provided feedback on the manuscript.

Conflict-of-interest disclosure: A.A.v.d.L. reports research funding from Roche, Bristol Myers Squibb (BMS), and Celgene; and reports membership on the board of directors or advisory committees of BMS and Celgene. F.T. reports membership on the board of directors of Novartis and AbbVie. M.G.D.P. reports honoraria from, and membership on the board of directors or advisory committees of BMS. P.F. reports consultancy with, and honoraria from and research funding from Novartis, AbbVie, Janssen, Jazz Pharmaceuticals, and BMS; and reports honoraria from French MDS Group. M.R.S. reports membership on the board of directors or advisory committees of Savona, AbbVie Inc, BMS, Geron Corporation, Forma Therapeutics, CTI BioPharma Corp, Karyopharm Therapeutics Inc, Novartis, Sierra Oncology, Inc, Taiho, Takeda Pharmaceutical, and TG Therapeutics Inc; reports consultancy with Forma Therapeutics Inc, Karyopharm Therapeutics Inc, Ryvu Therapeutics; is a current equity holder in publicly traded companies, Karyopharm Therapeutics Inc and Ryvu Therapeutics; received research funding from Takeda Pharmaceutical, TG Therapeutics Inc, ALX Oncology, Astex Pharmaceuticals, Incyte Corporation; and reports patents with, and royalties from, Boehringer Ingelheim. P.V. reports honoraria from BMS, Novartis, Pfizer, Incyte, Blueprint, and Stemline. I.K. reports consultancy with Novartis, BMS, Genesis, and AbbVie; received research funding from Novartis; and received honoraria from Genesis and AbbVie. V.S. reports membership on the board of directors or advisory committees of Santini, BMS, AbbVie, Geron, Gilead, CTI BioPharma, Otsuka, Servier, Janssen, and Syros. U.P. received research funding from Janssen Biotech, Geron, Fibrogen, Silence Therapeutics, Takeda, Curis, Merck, Servier, Syros, Novartis, Celgene, BMS, Amgen, Roche, Jazz Pharmaceuticals, and BeiGene; serves in a consulting role for Janssen Biotech, Geron, Silence Therapeutics, Takeda, Curis, Servier, Jazz Pharmaceuticals, Syros, AbbVie, Novartis, BMS, and Amgen; received honoraria from Silence Therapeutics, Celgene, Takeda, Servier, Jazz Pharmaceuticals, Syros, Novartis, and BMS; reports membership on the board of directors or advisory committees of MDS Foundation and BMS; and received other support (travel support and medical writing) from BMS. M.H. reports consultancy with Pfizer, PinotBio, AbbVie, Servier, BMS, Glycostem, Jazz Pharmaceuticals, Amgen, and Delbert Lab; received honoraria from Pfizer, Novartis, Sobi, Certara, Janssen, and Jazz

Pharmaceuticals; and received research funding from PinotBio, BerGenBio, Astellas, Agios, AbbVie, Loxo Oncology, BMS, Glycostem, Karyopharm, and Jazz Pharmaceuticals. M.T.V. serves on the advisory board of Jazz Pharmaceuticals, Celgene/BMS, and Syros; received research funding from Novartis and Celgene/BMS; and is a member of the speakers bureau of AstraZeneca, Novartis, AbbVie, Jazz Pharmaceuticals, Astellas, and Celgene/BMS. B.L.E. is a current equity holder in private company, Skyhawk Therapeutics, Exo Therapeutics, TenSixteen Bio, and Neomorph Inc; reports membership on the board of directors or advisory committees of Skyhawk Therapeutics, Exo Therapeutics, TenSixteen Bio, and Neomorph Inc; serves in a consulting role for AbbVie; and received research funding from Calico and Novartis. P.L.G. reports consultancy with, and research funding from BMS, Novartis, and Gilead. N.G. received research funding from Takeda; and honoraria from Novartis and BMS. E.P. is cofounder of, and holds a fiduciary role in a private company, Isabl Inc; and holds stock options in a private company, TenSixteen Bio. The remaining authors declare no competing financial interests.

ORCID profiles: E.B., 0000-0002-2057-7187; R.P.H., 0000-0002-7753-0697; P.L.G., 0000-0002-7615-9443; J.E.A.O., 0000-0003-1109-6178; M.C., 0000-0002-7629-0871; J.G.-A., 0000-0001-8863-5876; J.S.M.-M., 0000-0001-8444-153X; M.L., 0000-0001-5156-9086; N.F., 0000-0001-5355-7775; M.S., 0000-0001-7816-8071; M.J., 0000-0001-5217-3235; G.S., 0000-0002-2767-8191; M.Y.F., 0000-0001-6126-0859; A.P., 0000-0002-6122-0221; H.K.E., 0000-0002-6189-4752; C.G., 0000-0002-7566-5985; M.T., 0000-0002-3633-5852; L.P., 0000-0003-3176-6271; M.G.D.P., 0000-0002-6915-5970; M.B., 0000-0002-9158-881X; M.R.S., 0000-0003-3763-5504; F.P.S.S., 0000-0001-8573-9493; J.B., 0000-0002-4330-2928; I.K., 0000-0001-7668-0186; V.S., 0000-0002-5439-2172; F.S., 0000-0002-3251-2161; U.P., 0000-0003-1863-3239; M.H., 0000-0001-5318-9044; P.V., 0000-0003-0456-5095; C.F., 0000-0001-9372-1197; M.T.V., 0000-0002-6164-4761; L.-Y.S., 0000-0003-1866-7922; M.F., 0000-0002-5492-6349; B.L.E., 0000-0003-0197-5451; R.B., 0000-0002-5603-4598; L.M., 0000-0002-1460-1611; E.P., 0000-0003-1709-8983.

Correspondence: Elli Papaemmanuil, Department of Epidemiology and Biostatistics, Memorial Sloan Kettering Cancer Center, 321 E 61th St, New York, NY 10065; email: papaemme@mskcc.org.

Footnotes

Submitted 3 January 2024; accepted 5 June 2024; prepublished online on *Blood* First Edition 3 July 2024. <https://doi.org/10.1182/blood.2023023727>.

Deidentified patient data including clinical annotations and molecular data have been deposited to cBioPortal under the study name Myelodysplastic Syndrome International Working Group.

The online version of this article contains a data supplement.

There is a [Blood Commentary](#) on this article in this issue.

The publication costs of this article were defrayed in part by page charge payment. Therefore, and solely to indicate this fact, this article is hereby marked "advertisement" in accordance with 18 USC section 1734.

REFERENCES

1. Cazzola M. Myelodysplastic syndromes. *N Engl J Med*. 2020;383(14):1358-1374.
2. Papaemmanuil E, Gerstung M, Malcovati L, et al. Clinical and biological implications of driver mutations in myelodysplastic syndromes. *Blood*. 2013;122(22):3616-3699.
3. Haferlach T, Nagata Y, Grossmann V, et al. Landscape of genetic lesions in 944 patients with myelodysplastic syndromes. *Leukemia*. 2014;28(2):241-247.
4. Nazha A, Komrokji R, Meggendorfer M, et al. Personalized prediction model to risk stratify patients with myelodysplastic syndromes. *J Clin Oncol*. 2021;39(33):3737-3746.
5. Bersanelli M, Travaglino E, Meggendorfer M, et al. Classification and personalized prognostic assessment on the basis of clinical and genomic features in myelodysplastic syndromes. *J Clin Oncol*. 2021;39(11):1223-1233.
6. Kewan T, Durmaz A, Bahaj W, et al. Molecular patterns identify distinct subclasses of myeloid neoplasia. *Nat Commun*. 2023;14(1):3136.
7. Bernard E, Tuechler H, Greenberg PL, et al. Molecular international prognostic scoring system for myelodysplastic syndromes. *NEJM Evid*. 2022;1(7):EVID0a2200008.
8. Arber DA, Orazi A, Hasserjian R, et al. The 2016 revision to the World Health Organization classification of myeloid neoplasms and acute leukemia. *Blood*. 2016;127(20):2391-2405.

9. Arber DA, Orazi A, Hasserjian RP, et al. International consensus classification of myeloid neoplasms and acute leukemias: integrating morphologic, clinical, and genomic data. *Blood*. 2022;140(11):1200-1228.
10. Khoury JD, Solary E, Abla O, et al. The 5th edition of the World Health Organization classification of haematolymphoid tumours: myeloid and histiocytic/dendritic neoplasms. *Leukemia*. 2022;36(7):1703-1719.
11. Yoshizato T, Nannya Y, Atsuta Y, et al. Genetic abnormalities in myelodysplasia and secondary acute myeloid leukemia: impact on outcome of stem cell transplantation. *Blood*. 2017;129(17):2347-2358.
12. Bernard E, Nannya Y, Hasserjian RP, et al. Implications of TP53 allelic state for genome stability, clinical presentation and outcomes in myelodysplastic syndromes. *Nat Med*. 2020;26(10):1549-1556.
13. Papaemmanuil E, Gerstung M, Bullinger L, et al. Genomic classification and prognosis in acute myeloid leukemia. *N Engl J Med*. 2016;374(23):2209-2221.
14. Bernard E. R package for the IPSS-M. Accessed 16 August 2024. <https://github.com/papaemmelab/ipsm>
15. Smith AE, Kulasekararaj AG, Jiang J, et al. CSNK1A1 mutations and isolated del(5q) abnormality in myelodysplastic syndrome: a retrospective mutational analysis. *Lancet Haematol*. 2015;2(5):e212-e221.
16. Beauchamp EM, Leventhal M, Bernard E, et al. is mutated in clonal hematopoiesis and myelodysplastic syndromes and impacts RNA splicing. *Blood Cancer Discov*. 2021;2(5):500-517.
17. Okuda R, Nannya Y, Ochi Y, et al. Der(1;7)(q10;p10) presents with a unique genetic profile and frequent *ETNK1* mutations in myeloid neoplasms [abstract]. *Blood*. 2021;138(suppl 1):1513.
18. Gao T, Ptashkin R, Bolton KL, et al. Interplay between chromosomal alterations and gene mutations shapes the evolutionary trajectory of clonal hematopoiesis. *Nat Commun*. 2021;12(1):338.
19. Saiki R, Momozawa Y, Nannya Y, et al. Combined landscape of single-nucleotide variants and copy number alterations in clonal hematopoiesis. *Nat Med*. 2021;27(7):1239-1249.
20. Sanada M, Suzuki T, Shih L-Y, et al. Gain-of-function of mutated C-CBL tumour suppressor in myeloid neoplasms. *Nature*. 2009;460(7257):904-908.
21. Awada H, Nagata Y, Goyal A, et al. Invariant phenotype and molecular association of biallelic mutant myeloid neoplasia. *Blood Adv*. 2019;3(3):339-349.
22. Ilagan JO, Ramakrishnan A, Hayes B, et al. U2AF1 mutations alter splice site recognition in hematological malignancies. *Genome Res*. 2015;25(1):14-26.
23. Shiozawa Y, Malcovati L, Galli A, et al. Aberrant splicing and defective mRNA production induced by somatic spliceosome mutations in myelodysplasia. *Nat Commun*. 2018;9(1):3649.
24. Dalton WB, Helmenstine E, Pieterse L, et al. The K666N mutation in SF3B1 is associated with increased progression of MDS and distinct RNA splicing. *Blood Adv*. 2020;4(7):1192-1196.
25. Adema V, Khouri J, Ni Y, et al. Analysis of distinct hotspot mutations in relation to clinical phenotypes and response to therapy in myeloid neoplasia. *Leuk Lymphoma*. 2021;62(3):735-738.
26. Huber S, Haferlach T, Müller H, et al. MDS subclassification-do we still have to count blasts? *Leukemia*. 2023;37(4):942-945.
27. Makishima H, Saiki R, Nannya Y, et al. Germ line DDX41 mutations define a unique subtype of myeloid neoplasms. *Blood*. 2023;141(5):534-549.
28. Haase D, Stevenson KE, Neuberg D, et al. TP53 mutation status divides myelodysplastic syndromes with complex karyotypes into distinct prognostic subgroups. *Leukemia*. 2019;33(7):1747-1758.
29. Acha P, Mallo M, Solé F. Myelodysplastic syndromes with Isolated del(5q): Value of molecular alterations for diagnostic and prognostic assessment. *Cancers*. 2022;14(22):5531.
30. Woll PS, Kjällquist U, Chowdhury O, et al. Myelodysplastic syndromes are propagated by rare and distinct human cancer stem cells in vivo. *Cancer Cell*. 2014;25(6):794-808.
31. Malcovati L, Papaemmanuil E, Bowen DT, et al. Clinical significance of SF3B1 mutations in myelodysplastic syndromes and myelodysplastic/myeloproliferative neoplasms. *Blood*. 2011;118(24):6239-6246.
32. Malcovati L, Karimi M, Papaemmanuil E, et al. SF3B1 mutation identifies a distinct subset of myelodysplastic syndrome with ring sideroblasts. *Blood*. 2015;126(2):233-241.
33. Garcia-Gisbert N, Arenillas L, Roman-Bravo D, et al. Multi-hit TET2 mutations as a differential molecular signature of oligomonocytic and overt chronic myelomonocytic leukemia. *Leukemia*. 2022;36(12):2922-2926.
34. Sanada M, Uike N, Ohyashiki K, et al. Unbalanced translocation der(1;7)(q10;p10) defines a unique clinicopathological subgroup of myeloid neoplasms. *Leukemia*. 2007;21(5):992-997.
35. Ganster C, Müller-Thomas C, Haferlach C, et al. Comprehensive analysis of isolated der(1;7)(q10;p10) in a large international homogenous cohort of patients with myelodysplastic syndromes. *Genes Chromosomes Cancer*. 2019;58(10):689-697.
36. Galli A, Todisco G, Catamo E, et al. Relationship between clone metrics and clinical outcome in clonal cytopenia. *Blood*. 2021;138(11):965-976.
37. Meggendorfer M, Bacher U, Alpermann T, et al. SETBP1 mutations occur in 9% of MDS/MPN and in 4% of MPN cases and are strongly associated with atypical CML, monosomy 7, isochromosome i(17)(q10), ASXL1 and CBL mutations. *Leukemia*. 2013;27(9):1852-1860.
38. Gumari C, Pagliuca S, Prata PH, et al. Clinical and molecular determinants of clonal evolution in aplastic anemia and paroxysmal nocturnal hemoglobinuria. *J Clin Oncol*. 2023;41(1):132-142.
39. Pastor V, Hirabayashi S, Karow A, et al. Mutational landscape in children with myelodysplastic syndromes is distinct from adults: specific somatic drivers and novel germline variants. *Leukemia*. 2017;31(3):759-762.
40. Sahoo SS, Pastor VB, Goodings C, et al. Clinical evolution, genetic landscape and trajectories of clonal hematopoiesis in SAMD9/SAMD9L syndromes. *Nat Med*. 2021;27(5):1806-1817.
41. Lindsley RC, Mar BG, Mazzola E, et al. Acute myeloid leukemia ontogeny is defined by distinct somatic mutations. *Blood*. 2015;125(9):1367-1376.
42. Tazi Y, Arango-Ossa JE, Zhou Y, et al. Unified classification and risk-stratification in acute myeloid leukemia. *Nat Commun*. 2022;13(1):4622.
43. Cazzola M, Sehn LH. Developing a classification of hematologic neoplasms in the era of precision medicine. *Blood*. 2022;140(11):1193-1199.
44. Duncavage EJ, Bagg A, Hasserjian RP, et al. Genomic profiling for clinical decision making in myeloid neoplasms and acute leukemia. *Blood*. 2022;140(21):2228-2247.
45. Sirenko M, Bernard E, Creignou M, et al. *UBA1* mutations identify a rare but distinct subtype of myelodysplastic syndromes [abstract]. *Blood*. 2023;142(suppl 1):1862.
46. Lindsley RC, Saber W, Mar BG, et al. Prognostic mutations in myelodysplastic syndrome after stem-cell transplantation. *N Engl J Med*. 2017;376(6):536-547.
47. Weinberg OK, Siddon A, Madanat YF, et al. TP53 mutation defines a unique subgroup within complex karyotype de novo and therapy-related MDS/AML. *Blood Adv*. 2022;6(9):2847-2853.
48. Kuendgen A, Nomdedeu M, Tuechler H, et al. Therapy-related myelodysplastic syndromes deserve specific diagnostic sub-classification and risk-stratification-an approach to classification of patients with t-MDS. *Leukemia*. 2021;35(3):835-849.
49. Aguirre LE, Al Ali N, Sallman DA, et al. Assessment and validation of the molecular international prognostic scoring system for myelodysplastic syndromes. *Leukemia*. 2023;37(7):1530-1539.
50. Palomo L, Meggendorfer M, Hutter S, et al. Molecular landscape and clonal architecture of adult myelodysplastic/myeloproliferative neoplasms. *Blood*. 2020;136(16):1851-1862.

51. Geissler K, Jäger E, Barna A, et al. Correlation of RAS-pathway mutations and spontaneous myeloid colony growth with progression and transformation in chronic myelomonocytic leukemia—a retrospective analysis in 337 patients. *Int J Mol Sci.* 2020;21(8):3025.
52. Carr RM, Vorobyev D, Lasho T, et al. RAS mutations drive proliferative chronic

myelomonocytic leukemia via a KMT2A-PLK1 axis. *Nat Commun.* 2021;12(1):2901.

53. Papaemmanuil E, Döhner H, Campbell PJ. Genomic classification in acute myeloid leukemia. *N Engl J Med.* 2016;375(9):900-901.
54. Bolton KL, Ptashkin RN, Gao T, et al. Cancer therapy shapes the fitness landscape of clonal

hematopoiesis. *Nat Genet.* 2020;52(11):1219-1226.

© 2024 American Society of Hematology. Published by Elsevier Inc. Licensed under [Creative Commons Attribution-NonCommercial-NoDerivatives 4.0 International \(CC BY-NC-ND 4.0\)](#), permitting only noncommercial, nonderivative use with attribution. All other rights reserved.